Elsevier Editorial System(tm) for Clinical Biomechanics
Manuscript Draft

Manuscript Number: CLBI-D-14-00503R2

Title: The biomechanical characteristics of wearing FitFlop™ sandals highlight significant alterations in gait pattern: A comparative study.

Article Type: Research Paper

Keywords: Gait; Instability; Footwear; Joint Moment.

Corresponding Author: Dr. Darren C James,

Corresponding Author's Institution: London South Bank University

First Author: Darren C James

Order of Authors: Darren C James; Laura J Farmer; Jason B Sayers; David P Cook; Katya N Mileva

Abstract: Background: The net contribution of all muscles that act about a joint can be represented as an internal joint moment profile. This approach may be advantageous when studying footwear-induced perturbations during walking since the contribution of the smaller deeper muscles that cross the ankle joint cannot be evaluated with surface electromyography. Therefore, the present study aimed to advance the understanding of FitFlop™ footwear interaction by investigating lower extremity joint moment, and kinematic and centre of pressure profiles during gait.
Methods: 28 healthy participants performed 5 walking trials in 3 conditions: a FitFlop™ sandal, a conventional sandal and an athletic trainer. Three-dimensional ankle joint, and sagittal plane knee and hip joint moments, as well as corresponding kinematics and centre of pressure trajectories were evaluated.
Findings: FitFlop™ differed significantly to both the conventional sandal and athletic trainer in: average anterior position of centre of pressure trajectory ($P<0.0001$) and peak hip extensor moment ($P=0.001$) during early stance; average medial position of centre of pressure trajectory during late stance; peak ankle dorsiflexion and corresponding range of motion; peak plantarflexor moment and total negative work performed at the ankle (all $P<0.0001$).
Interpretation: The present findings demonstrate that FitFlop™ footwear significantly alters the gait pattern of wearers. An anterior displacement of the centre of pressure trajectory during early stance is the primary response to the destabilising effect of the mid-sole technology, and this leads to reductions in sagittal plane ankle joint range of motion and corresponding kinetics. Future investigations should consider the clinical implications of these findings.

***Highlights (for review)**

Highlights

- Gait was investigated in people wearing FitFlop™ footwear.
- An early change in centre of pressure location is the primary response.
- The sagittal plane ankle moment and range of motion are reduced throughout stance.
- These findings may have clinical relevance.

The biomechanical characteristics of wearing FitFlop™ sandals highlight significant alterations in gait pattern: A comparative study.

Darren C. James [a], Laura J. Farmer [a], Jason B. Sayers [a], David P. Cook [a], Katya N. Mileva [a]

[a] Sport & Exercise Science Research Centre, School of Applied Sciences, London South Bank University, London, UK.

Keywords: Gait, Instability, Footwear, Joint Moment.

Corresponding author:

Dr Darren James

School of Applied Sciences, ESBE

London South Bank University

103 Borough Road, London, SE1 0AA, UK.

Email: jamesd6@lsbu.ac.uk

TEL: +44 (0)207 815 7992

Word Count:

Abstract: 251

Main Text: 4,199

Abstract

Background: The net contribution of all muscles that act about a joint can be represented as an internal joint moment profile. This approach may be advantageous when studying footwear-induced perturbations during walking since the contribution of the smaller deeper muscles that cross the ankle joint cannot be evaluated with surface electromyography. Therefore, the present study aimed to advance the understanding of FitFlop™ footwear interaction by investigating lower extremity joint moment, and kinematic and centre of pressure profiles during gait.

Methods: 28 healthy participants performed 5 walking trials in 3 conditions: a FitFlop™ sandal, a conventional sandal and an athletic trainer. Three-dimensional ankle joint, and sagittal plane knee and hip joint moments, as well as corresponding kinematics and centre of pressure trajectories were evaluated.

Findings: FitFlop™ differed significantly to both the conventional sandal and athletic trainer in: average anterior position of centre of pressure trajectory (P<0.0001) and peak hip extensor moment (P=0.001) during early stance; average medial position of centre of pressure trajectory during late stance; peak ankle dorsiflexion and corresponding range of motion; peak plantarflexor moment and total negative work performed at the ankle (all P<0.0001).

Interpretation: The present findings demonstrate that FitFlop™ footwear significantly alters the gait pattern of wearers. An anterior displacement of the centre of pressure trajectory during early stance is the primary response to the destabilising effect of the mid-sole technology, and this leads to reductions in sagittal plane ankle joint range of motion and corresponding kinetics. Future investigations should consider the clinical implications of these findings.

1. Introduction

Technology-inspired footwear aims to offer advantages in sporting performance, restore ‘natural’ foot function and promote well-being, as well as assist mobility in a number of pathological conditions. In the last decade instability shoes have come to the fore under the premise that lower extremity muscles can be trained when the musculoskeletal system is functionally destabilised by a midsole-induced perturbation (Nigg et al., 2006). In principle, this concept is well-founded since traditional balance training is known to induce sensorimotor adaptations that result in spinal and supraspinal neural reorganisation (Taube et al., 2008). Accordingly, balance training strategies are used not just for rehabilitation but also for improving muscle performance by stressing the musculotendinous system (Taube et al., 2008).

However, the evidence that instability shoes enhance muscle activation profiles during walking when compared to a control shoe is equivocal. Indeed, some studies have shown Masai Barefoot Technology® (MBT®), the most notable unstable shoe concept, to significantly increase muscle (m.) gastrocnemius activation amplitude during loading response of the gait cycle when compared to conventional footwear (Price et al., 2013; Romkes et al., 2006); whereas others have not (Branthwaite et al., 2013; Nigg et al., 2006). Similar observations have been demonstrated in muscles from the quadriceps group (Branthwaite et al., 2013; Nigg et al., 2006; Price et al., 2013; Romkes et al., 2006) and in m. peroneus longus activity (Branthwaite et al., 2013; Price et al., 2013) throughout the gait cycle. Despite this lack of consensus, there is increasing belief, substantiated from findings on static balance control (Coza et al., 2009; Landry et al., 2010), that unstable footwear activates the smaller muscles crossing the ankle joint more so than conventional or athletic footwear (Burgess and Swinton, 2012; Maffiiuletti, 2012; Nigg et al., 2012).

The FitFlop™ sandal is an innovative form of unstable footwear. The concept underpinning this footwear, Microwobbleboard™ technology, is a column based triple density midsole design (Fig. 1A) intended to induce a movement strategy in such a way that facilitates the second ankle rocker process (Perry and Burnfield, 2010). In principle, this should evoke enhanced activity from the stabilising leg muscles through the moderate medio-lateral (M-L) destabilising effect afforded by the midsole construction. FitFlop™ interaction has been reported to effectively apply frontal plane instability (Price et al., 2013); however, there is no published evidence so far of enhanced muscle activation profiles unique to this midsole technology (Burgess and Swinton, 2012; Price et al., 2013).

All extrinsic muscles that cross the ankle joint are potentially involved in controlling perturbations during gait (Nigg et al., 2012), but the contribution from all participating muscles cannot be evaluated due to the inherent difficulty associated with the acquisition of electromyographic (EMG) activation profiles from the smaller, deeper-lying muscles (Kamen and Caldwell, 1996). Instead, the internal joint moment profile can be used to represent the net contribution of all muscles that act about a joint (Lloyd and Besier, 2003). Calculations using an inverse dynamics approach, which derives a joint moment profile from movement kinematics and ground reaction forces, may prove successful in understanding FitFlop™ interaction further. Currently, no information regarding lower extremity joint kinetics has been forthcoming in the literature with respect to this footwear, and investigation is therefore warranted. Consequently, the purpose of the present study was to compute and compare lower extremity joint moment profiles during walking in three different types of footwear: a FitFlop™ sandal, a comparative sandal and a standard athletic trainer. Joint angular kinematics and centre of pressure (COP) trajectory were also assessed for differences due to footwear. Based on the properties of the Microwobbleboard™ technology, and the ineffectiveness of soft mid-sole constructions to produce reactive forces (Perry et al., 2007), it was hypothesised that wearing FitFlop™ sandals would significantly change the anterior-posterior COP trajectory during early stance, due to altered lower limb net joint moment profiles. Consequently, kinematic alterations in gait were anticipated. The results from this study may help to inform health practitioners of the functional adaptations imposed on the wearer by the FitFlop™ sandal when prescribing technology-inspired footwear for assistive mobility.

2. Methods

2.1 Participants

Twenty eight healthy individuals, 13 males (mean (SD): 28.8 (8.8) years, 78.0 (12.1) kg, 1.74 (0.07) m) and 15 females (mean (SD): 31.2 (7.3) years, 64.4 (4.9) kg, 1.65 (0.04) m) were informed of the testing procedures and provided written informed consent to participate in the study. Prior approval was received from the local University Research Ethics Committee (UREC 1021). Participants reported to be in good health and free from any recent orthopaedic trauma, underlying pathology or neurological problems.

Sample size estimation ($P<0.05$, $\beta=0.20$) was based on ankle joint angular (plantarflexor) impulse ($Nm/Kg.s^{-1}$) data from a pilot trial investigating FitFlop™ footwear. The angular impulse represents the angular moment of force acting over a specified period of time and provides a useful concept for understanding loading rate (Stefanyshyn et al., 2006). In the context of the present study, it allows differentiation of the impact of footwear on joint energetics.

2.2 Experimental design

Three dimensional (3-D) lower extremity kinematics and force data were measured in three conditions: a FitFlop™ Walkstar sandal (FF), a market comparative sandal (Birkenstock® Gizeh; BIRK), and a standard commercially-available athletic trainer free from any technological construct (Decathlon Kalenji Success, 0.39 EVA, Shore 55C, KAL)(Fig. 1B). Windows were cut into the trainers so that an exact representation of 3-D position data of the foot segment could be collected. The testing protocol consisted of five repeated walking trials in each condition at individually-preferred walking speed. This speed was determined prior to the commencement of the protocol as a range for each participant to walk within based on their average speed (SD 5%) from five trials recorded in the KAL condition. Condition trials were randomised to exclude any potential order effect. The participants were given sufficient time to familiarise walking in each condition and to establish their starting position so that a right foot contact was made on an embedded force platform corresponding to at least the sixth step from gait initiation. This is well beyond the time required to elicit a steady state walking pattern (Couillandre and Breniere, 2003).

2.3 Data acquisition and processing

Kinematic data were acquired using an eight camera 3-D motion analysis system (Oqus 3-series, Qualisys AB, Sweden), sampled at 120Hz and synchronously collected with force platform data (type 9281E, Kistler, UK) at 2040Hz. Since gait in healthy subjects is considered generally symmetrical at preferred walking speed (Seeley, Umberger, & Shapiro, 2008), only data from the right extremity were entered for statistical analysis. This approach is consistent with the related literature (Burgess and Swinton, 2012; Branthwaite et al., 2013; Nigg et al., 2006; Price et al., 2013; Romkes et al., 2006).

The 3-D pose of seven body segments of the lower extremity (pelvis; left and right thighs; left and right shanks; both feet) were reconstructed by tracking the trajectories of 26 retro-reflective spherical markers mounted in accordance with an accepted six degree-of-freedom marker set (6DOF, (Cappozzo et al., 1995). A further 18 markers were placed bilaterally on anatomical landmarks during a static barefoot calibration, in order to define each segment’s local coordinate system (Cappozzo et al., 1995; Collins et al., 2009; Leardini et al., 2007). These were subsequently removed prior to the dynamic trials so that 6DOF joint movement was expressed relative to the ‘calibrated anatomical systems technique’ (Cappozzo et al., 1995).

2.3.1 Joint kinematics.

Raw marker trajectories and ground reaction force (GRF) data were exported into Visual 3D software (C-Motion Inc., USA) and smoothed with a 10Hz and 25Hz 4th order low-pass Butterworth filter, respectively. Joint rotations were calculated using an X (sagittal), Y (frontal), Z (transverse) Cardan rotation sequence and were referenced to coordinate systems embedded in the distal segment, such that ankle dorsiflexion (DF), adduction (ADD) (commonly referred to as inversion), and internal rotation (INT) were positive. Only sagittal plane rotations were reported at the knee and hip joints, thus a positive rotation reflects extension (KE) and flexion (HF), respectively. 3-D ankle joint range of motion (ROM, °): peak plantarflexion (PF)-DF, peak abduction (ABD)-ADD, peak external rotation (EXT)-INT; and sagittal plane knee (initial contact (IC)-peak knee flexion (KF)) and hip (IC-peak hip extension (HE)) joint ROM, and the respective peak angles (°) were derived from stance phase of the gait cycle. Stance time and step length were also extracted for statistical analysis.

2.3.2 Joint kinetics.

A Newton-Euler inverse dynamics approach was employed to calculate the 3-D internal moments acting about the lower extremity joints. Again, only sagittal plane moments were reported from the knee and hip joints. The moments were expressed relative to a distal anatomical frame of reference and normalised to bodyweight (Nm/kg). The respective peaks, times (% stance) and overall joint angular impulse (Nm/kg.s^{-1}) were derived during stance phase. Also, ankle joint power, representing the sum of powers within the segment coordinate system, was used to express the total negative and positive periods within the signal as an indication of the total work (J.kg^{-1}) performed at the joint.

2.3.3 Centre of pressure (COP).

The COP trajectory was resolved into a virtual foot local coordinate system from contact with the force platform (Visual3D, C-Motion Inc., USA). Specifically, the forward progression COP was normalised (arbitrary unit, a.u) by the distance along the anterior-posterior (A-P) axis from the proximal end of the foot segment (ankle joint) to the 2nd metatarsal head (distal joint centre) (O'Connell et al., 1998). This meant that A-P COP range of motion was quantified on the order of -1 to 2, where a negative value indicates that COP is behind the ankle joint centre and a value > 1 reflects COP ahead of the metatarsals (O'Connell et al., 1998). Similarly, the medio-lateral (M-L) COP was normalised (a.u) by its distance along the distal radius of the foot segment (1st to 5th metatarsal head) with respect to the longitudinal axis of the foot segment. An M-L COP equal to zero reflects a position located on the A-P axis, whereas a positive value indicates a laterally-directed trajectory (Visual3D, C-Motion Inc., USA). The data were expressed relative to subdivisions of stance phase, representing early (0-33%; COP33), mid- (34-66%; COP66) and late stance (67-100%; COP100) regions (Chang et al., 2008).

2.4 Statistical analysis

All outcome variables were determined for each of five trials completed by the participant in each condition, averaged, and then compared across conditions. All data were confirmed as being normally distributed (Kolmogorov-Smirnov 1-sample test, PASW v18.0, IBM Corp., USA), hence a single factor (condition: FF vs BIRK vs KAL) repeated measures ANOVA was used to identify main and evaluate the effect sizes ($ŋ^2$). *Post-hoc* Holm-Sidak corrections were applied for pair-wise comparisons and statistically significant differences were accepted when $P<0.05$.

3. Results

There was no significant difference in walking speed ($P>0.05$) between conditions (mean (SD); KAL: 1.45 (0.15) m/s; BIRK: 1.44 (0.15) m/s; FF: 1.44 (0.14) m/s).

3.1 Joint kinematics

Mean (n=28) joint angular kinematic profiles are presented in Figure 2. Condition effects were found at the ankle and knee joints and Table 1 highlights where significant differences from the pair-wise comparisons existed. At the ankle joint, there were significant amplitude differences in peak plantarflexion during early stance ($F_{(2, 54)}=55.5$, $P<0.0001$, $ŋ^2=0.67$), and peak dorsiflexion ($P<0.0001$, $ŋ^2=0.76$), adduction ($P<0.0001$, $ŋ^2=0.28$) and internal rotation ($P=0.001$, $ŋ^2=0.23$) during late stance. There were significant differences in ankle ROM measured in all three planes: PF-DF ($P<0.0001$, $ŋ^2=0.49$), ABD-ADD ($P<0.0001$, $ŋ^2=0.30$) and EXT-INT ($P<0.0001$, $ŋ^2=0.25$).

At the knee, there was a significant difference in peak knee flexion in stance ($P<0.0001$, $\eta^2=0.37$) and ROM ($P=0.002$, $\eta^2=0.21$). No significant differences ($P>0.05$) were found at the hip joint between conditions and comparable stance time and step length measures ($P>0.05$) were observed.

3.2 Joint kinetics

Mean ($n=28$) joint moment ensemble profiles are presented in Figure 3. Condition effects were found at all joints and Table 2 highlights where significant findings from the pair-wise comparisons existed. At the ankle joint there were significant differences in the peak DF moment ($P=0.001$, $\eta^2=0.23$) and time ($P<0.0001$, $\eta^2=0.50$), the peak PF moment ($P<0.0001$, $\eta^2=0.42$); and for the overall sagittal plane impulse ($P<0.0001$, $\eta^2=0.37$). In the frontal plane, there were significant differences in the peak ADD moment ($P<0.0001$, $\eta^2=0.30$) and time ($P=0.007$, $\eta^2=0.13$); and for the overall frontal plane impulse ($P<0.0001$, $\eta^2=0.34$). In the transverse plane, there were significant differences in the peak EXT moment ($P=0.019$, $\eta^2=0.14$) and time ($P<0.0001$, $\eta^2=0.35$); and for the overall transverse plane impulse ($P=0.014$, $\eta^2=0.15$). Additionally, the total negative ($P<0.0001$, $\eta^2=0.61$) and positive ($P=0.002$, $\eta^2=0.20$) work performed about the ankle joint was also significantly different between conditions.

At the knee, there were significant differences in the peak KE moment ($P<0.0001$, $\eta^2=0.28$) and time ($P=0.001$, $\eta^2=0.28$); and the peak KF moment ($P<0.0001$, $\eta^2=0.30$). At the hip, there were significant differences in the peak HE moment ($P=0.001$, $\eta^2=0.24$), the peak HF moment ($P<0.0001$, $\eta^2=0.41$) and time ($P=0.006$, $\eta^2=0.18$); and for the overall sagittal plane impulse ($P=0.025$, $\eta^2=0.13$).

3.3 Centre of Pressure

A condition effect was found for A-P COP trajectory during early stance ($P<0.0001$, $\eta^2=0.39$). Specifically, in the FF condition the COP was significantly anterior compared to both KAL ($P<0.0001$) and BIRK ($P<0.0001$) (Fig. 4). No differences were evident between conditions during mid-stance ($P>0.05$). In late stance a condition effect was again noted ($P=0.025$, $\eta^2=0.16$), but the difference reached significance only between KAL and BIRK conditions ($P<0.0001$).

Similarly, condition effects were also evident during early ($P=0.033$, $\eta^2=0.12$) and late stance ($P<0.0001$, $\eta^2=0.54$) in the M-L direction. Specifically, FF COP was significantly lateral than BIRK COP ($P=0.013$) during early stance, and significantly medial to both KAL ($P=0.023$) and BIRK ($P<0.0001$) COP during late stance (Fig. 4).

4. Discussion

The purpose of the present study was to evaluate the biomechanical characteristics of gait whilst walking in FitFlop™ footwear (FF). Comparisons were made against a conventional sandal (BIRK) and a standard athletic trainer (KAL). Amongst the numerous significant pair-wise differences reported in this study, there were four main findings. When compared to both BIRK and KAL conditions, FF interaction results in: 1) a greater anterior displacement of the average COP trajectory during early stance; 2) a greater medial displacement of the average COP trajectory during late stance; 3) an increased peak hip extensor moment during early stance; and 4) a reduction in sagittal plane ankle joint range of motion throughout stance phase. In regard to (4) there is a corresponding reduction in torque about the ankle joint and in the total negative work performed at this joint throughout stance phase. Combined, these main findings indicate that FFs alter an individual’s gait pattern significantly, which corroborates our experimental hypothesis.

Microwobbleboard™ technology, the central technology underpinning FitFlop™ footwear, was designed to project the wearer into the middle section of the foot-bed (the softer, “questioning” zone) earlier in stance phase than conventional footwear. The anterior displacement of the COP trajectory during early stance, compared to both KAL and BIRK, demonstrates that this objective has been successfully translated into a feature of gait whilst wearing FF. This result, however, is in disagreement with the findings of Price et al. (2013) who reported no shift in A-P COP trajectory for FF wearers. Instability in FitFlop™ footwear was designed to be phase-dependent within the stance phase rather than across the whole period of stance. Price and colleagues do not take account of this. Indeed, in the present study A-P COP trajectory was shown to be different between conditions during early but not during mid-stance. This means that forward progression was impeded during the transition between early and mid-stance in the FF condition. Most likely this is caused by the softer middle section of the foot-bed in FitFlop™ footwear. Expressing the COP trajectory relative to the entire stance duration does not provide a sufficiently detailed representation of FF-interaction dynamics, and important features of interaction may well be masked by such an approach.

The location of COP under the foot is a direct reflection of the neural control of the ankle muscles (Winter, 1995). The more anteriorly directed average COP trajectory observed in FF during early stance likely results from a reduced internal ankle dorsiflexion moment for this footwear (Table 2). The magnitude of this moment determines the quantity of trunk energy to be re-distributed to distal segments for effective deceleration during loading response (Siegel et al., 2004). Hence this finding implies that for FF the second ankle rocker is achieved earlier and a greater time is spent in single limb support. The unaltered average A-P COP trajectory during mid-stance and the comparable stance phase durations between conditions indirectly support this view. However, a reduced internal dorsiflexor moment during loading response is an inherent characteristic of open-heel footwear designs (Zhang et al., 2013). The present results show this is not the case whilst wearing a BIRK sandal. We believe that the rigid construction of the BIRK sandal impedes forward progression during early stance. In contrast to FF, a greater frontal plane internal adductor moment acting about the ankle joint was evident, which likely reflects a control exerted by BIRK for 'over-pronation'. If this is true, then enhanced contribution from the plantarflexor muscles is required to accelerate the body's centre of mass (Wang and Gutierrez-Farewik, 2011). Whilst this cannot be supported directly, we did observe significantly higher sagittal plane angular impulse and total positive work performed about the ankle joint in the BIRK condition (Table 2). Moreover, the peak internal knee extensor moment, at approximately 20% of stance phase, was also higher. The magnitude of this moment is negatively correlated with A-P COP forward displacement (r=-0.62; P=0.006) (Shimokochi et al., 2009). This suggests inefficiency in weight transfer from early stance to mid-stance whilst wearing a conventional sandal compared to FitFlop™ footwear.

The medio-lateral (M-L) destabilisation resulting from interaction with the FitFlop™ mid-sole construction is expected to result in enhanced activity of stabilising leg musculature. In the present study, this consideration is investigated by way of the observed changes in the net joint moments to account for the contribution of all muscles that act about a lower extremity joint. We opted for this approach rather than using EMG since the smaller deeply located muscles which may contribute to the control for a footwear-induced perturbation are inaccessible with surface EMG electrodes. Whilst increased muscle activation cannot be specifically revealed from the present findings, the joint moment data (limitations accepted) provide evidence of greater reliance on the hip extensors for support and stabilisation when wearing FFs than for comparative footwear. A greater internal hip extensor moment was observed during early stance in the FF condition compared to both BIRK and KAL conditions. The time at which this occurred corresponded to approximately 10% of stance phase, which is the period when COP in the FF condition was found to be more anteriorly displaced. This may explain the subsequent impediment to A-P COP displacement in mid-stance as a means of preserving the overall support moment (Winter, 1980). Interestingly, from the present study, the amplitudes of peak hip extensor moments appear inversely related to the amplitudes of the subsequent peak knee extensor moments (Table 2, all conditions). Shimokochi et al. (2009) have demonstrated such a relationship (r=-0.66, P=0.003) for the support phase of a single limb landing task. Hence, it appears that wearing FitFlop™ footwear alters lower extremity joint contributions: FF favours a support moment strategy for the hip, whereas BIRK and KAL favour support moments for the knee.

Evidence published so far cannot confirm increased activation of the larger muscles of the lower extremity whilst walking in FitFlop™ footwear (Burgess and Swinton, 2012; Price et al., 2013). The results of Burgess and Swinton (2012) should be interpreted with caution, since placing a restriction on participant walking speed (1.34 m/s) does not appear to be ecologically valid given natural variation between subjects. Nonetheless, in their discussion Burgess and Swinton (2012) allude to the potential for increased activation of the smaller, deeper-lying muscles that act about the ankle joint whilst wearing FitFlop. Similar opinion has been expressed in the literature with respect to instability shoes more generally (Nigg et al., 2012). These muscles acting across the ankle joint complex react more quickly to frontal and transverse plane changes in joint position than the larger muscles that ostensibly control for sagittal plane deviations (Nigg et al., 2012). Joint stability is achieved with low levels of torque, since these muscles have smaller moment arms. The reduction in peak internal ankle plantarflexor moment observed in the FF condition and the subsequent kinematic adaptations are potentially a consequence of a greater reliance placed on the smaller muscles crossing the ankle joint. Until EMG investigations using indwelling electrodes or highly-selective surface EMG array techniques (Coza et al., 2009) are available for dynamics studies this will remain conjecture.

The most notable alteration to gait pattern observed with FitFlop™ in the present study, was a reduction in peak ankle dorsiflexion angle (Table 1). The effect size for our cohort was 76%. Whilst the participants in this study had ‘normal’ gait, the clinical implications of this finding are worthy of mention. For example, reduced ankle dorsiflexor range of motion is an important risk factor for individuals suffering from plantar fasciitis, the most common foot-related disorder treated by healthcare professionals (McPoil et al., 2008). Reducing sagittal plane ankle joint ROM and the corresponding net rotational peak force acting about this joint during stance phase may be an effective method of reducing pain for these sufferers. Price et al. (2013), however, found no differences in sagittal plane ankle joint kinematics in their comparison of FitFlop™ and alternative instability footwear. . It is noteworthy that these authors used a static neutral configuration prior to dynamic trials for each condition. The present study, in contrast, performed this calibration only once during barefoot standing, representing a global neutral configuration. This may explain the lack of coherence in significant kinematic findings between the respective two studies.

Finally, we observed a significantly more medial COP trajectory during late stance in the FF condition than in both KAL and BIRK. This matches expectations since all supinatory rotations about the ankle joint (dorsiflexion, adduction and internal rotation) were significantly restricted during the latter part of stance for participants wearing the FitFlop™ sandal. It is noteworthy that there was no difference in peak adduction between FF and

BIRK, but there was significantly greater transverse plane ankle joint motion in BIRK. The latter is likely a compensation strategy imposed by the inherently stiff construction of the BIRK sandal and this offsets the lack of frontal plane motion related to the foot-bed. The present M-L COP data indicate that a greater range of motion was present in the FF condition (Fig. 4). Similar findings have been presented by others for unstable footwear (Stoggl et al., 2010; Zhang et al., 2012). If soft mid-sole constructions like that for FitFlop™ impair M-L balance control (Perry et al., 2007), a mechanical balance control response would be expected to allow unhindered forward progression. Indeed, Price et al. (2013) were able to demonstrate a significantly greater m.peroneus longus (PL) activity during pre-swing in the FitFlop™ condition compared to other instability shoes. They did not, however, record any concomitant differences between conditions in M-L COP range of motion. Unfortunately, the only other FitFlop™ investigation Burgess and Swinton (2012) excluded PL activation from their analysis and they reported no differences in activation profiles of the larger lower extremity muscles. Future studies incorporating advanced EMG analysis may help to understand the precise muscular responses to the perturbation induced by FitFlop™ footwear.

This study is not without limitations. The inverse dynamics procedure used to calculate the net joint moments has a number of shortcomings, which can arise from errors in basic methodological experimental procedures. For example, inaccuracies in ground reaction force measurements and estimation of centre of pressure location; marker positioning, selection of an appropriate technical frame of reference and skin movement artefact are all significant contributors to the uncertainty in joint rotational force estimates derived through this process (Riemer et al., 2008). Validation of the accuracy of the force platforms in 3-D space, as performed in our Laboratory, overcomes the main sources of error relating to joint moment calculation. Furthermore, all experimental conditions were performed by each participant on the same day, which minimizes the potential error due to marker placement.

Finally, the errors associated with joint centre estimation and segmental motion tracking during dynamic trials, were considered by adopting the CAST technique (Cappozzo et al., 1995; Collins et al., 2009). Such steps remove the major experimentally-induced limitations associated with the inverse dynamics procedure and give confidence in the reliability of the study outcomes.

5. Conclusion

The present study has demonstrated that FitFlop™ footwear significantly alters gait pattern for the wearers. The primary biomechanical response to the destabilising effect of the mid-sole Microwobbleboard™ technology was the anterior displacement of the centre of pressure trajectory. Stability, in preparation for mid-stance, appears to be consolidated through larger net sagittal plane rotational forces about the hip. Consequently, the ankle joint range of motion, the magnitude of peak dorsiflexion and the net rotational forces acting about the ankle are reduced. This lowers the amount of work performed at the ankle joint during support and propulsion.. These findings warrant future work to determine the potential clinical benefits from reducing the ankle joint loading associated with walking in FitFlop™ footwear.

Acknowledgement

The authors would like to thank Dr. John Seeley for his assistance during the revision process of this manuscript.

Conflict of Interest

Drs. Cook and James developed the Microwobbleboard™ technology concept in 2006 and Dr Cook is the named researcher on the patent, but without ownership of the intellectual property. Between 2006-2013 London South Bank University and FitFlop Ltd. had a contractual agreement in place for testing of FitFlop™ footwear. Drs Cook, James, or London South Bank University receive no royalties for the commercial success of the product. The present study was designed, analysed and the manuscript written by the authors with no influence from the FitFlop Ltd.

References

Branthwaite, H., Chockalingam, N., Pandyan, A., Khatri, G., 2013. Evaluation of lower limb electromyographic activity when using unstable shoes for the first time: a pilot quasi control trial. Prosthet. Orthot. Int. 37, 275-281.

Burgess, K.E., Swinton, P.A., 2012. Do Fitflops increase lower limb muscle activity? Clin. Biomech. 27, 1078-1082.

Cappozzo, A., Catani, F., Croce, U.D., Leardini, A., 1995. Position and orientation in space of bones during movement: anatomical frame definition and determination. Clin. Biomech. 10, 171-178.

Chang, R., Van Emmerik, R., Hamill, J., 2008. Quantifying rearfoot-forefoot coordination in human walking. J. Biomech. 41, 3101-3105.

Collins, T.D., Ghoussayni, S.N., Ewins, D.J., Kent, J.A., 2009. A six degrees-of-freedom marker set for gait analysis: repeatability and comparison with a modified Helen Hayes set. Gait Posture. 30, 173-180.

Couillandre, A., Breniere, Y., 2003. How does the heel-off posture modify gait initiation parameter programming? J. Mot. Behav. 35, 221-227.

Coza,A.,von Tscharner,V.,Nigg,B.M., 2009. Activity mapping of lower leg muscles using a circumferential electrode array. Footwear Sci. 1, 135-143.

Kamen, G., Caldwell, G.E., 1996. Physiology and interpretation of the electromyogram. J. Clin. Neurophysiol. 13, 366-384.

Landry, S.C., Nigg, B.M., Tecante, K.E., 2010. Standing in an unstable shoe increases postural sway and muscle activity of selected smaller extrinsic foot muscles. Gait Posture. 32, 215-219.

Leardini, A., Benedetti, M.G., Berti, L., Bettinelli, D., Nativo, R., Giannini, S., 2007. Rear-foot, mid-foot and fore-foot motion during the stance phase of gait. Gait Posture. 25, 453-462.

Lloyd, D.G., Besier, T.F., 2003. An EMG-driven musculoskeletal model to estimate muscle forces and knee joint moments in vivo. J. Biomech. 36, 765-776.

Maffiiuletti, N.A., 2012. Increased lower limb muscle activity induced by wearing MBT shoes: physiological benefits and potential concerns. Footwear Sci. 4, 123-129.

McPoil, T.G., Martin, R.L., Cornwall, M.W., Wukich, D.K., Irrgang, J.J., Godges, J.J., 2008. Heel pain--plantar fasciitis: clinical practice guildelines linked to the international classification of function, disability, and health from the orthopaedic section of the American Physical Therapy Association. J. Orthop. Sports Phys. Ther. 38, A1-A18.

Nigg, B., Federolf, P.A., von Tscharner, V., Nigg, S., 2012. Unstable shoes: functional concepts and scientific evidence. Footwear Sci. 4, 73-82.

Nigg, B., Hintzen, S., Ferber, R., 2006. Effect of an unstable shoe construction on lower extremity gait characteristics. Clin. Biomech. 21, 82-88.

O'Connell, P.G., Lohmann Siegel, K., Kepple, T.M., Stanhope, S.J., Gerber, L.H., 1998. Forefoot deformity, pain, and mobility in rheumatoid and nonarthritic subjects. J. Rheumatol. 25, 1681-1686.

Perry, J., Burnfield, J.M., 2010. Gait analysis: normal and pathological function, 2nd ed. SLACK, Thorofare, NJ.

Perry, S.D., Radtke, A., Goodwin, C.R., 2007. Influence of footwear midsole material hardness on dynamic balance control during unexpected gait termination. Gait Posture. 25, 94-98.

Price, C., Smith, L., Graham-Smith, P., Jones, R., 2013. The effect of unstable sandals on instability in gait in healthy female subjects. Gait Posture. 38, 410-415.

Riemer, R., Hsiao-Wecksler, E.T., Zhang, X., 2008. Uncertainties in inverse dynamics solutions: a comprehensive analysis and an application to gait. Gait Posture. 27, 578-588.

Romkes, J., Rudmann, C., Brunner, R., 2006. Changes in gait and EMG when walking with the Masai Barefoot Technique. Clin. Biomech. 21, 75-81.

Seeley, M.K., Umberger, B.R., Shapiro, R., 2008. A test of the functional asymmetry hypothesis in walking. Gait Posture. 28, 24-28.

Shimokochi, Y., Yong Lee, S., Shultz, S.J., Schmitz, R.J., 2009. The relationships among sagittal-plane lower extremity moments: implications for landing strategy in anterior cruciate ligament injury prevention. J. Athl Train. 44, 33-38.

Siegel, K.L., Kepple, T.M., Stanhope, S.J., 2004. Joint moment control of mechanical energy flow during normal gait. Gait Posture. 19, 69-75.

Stefanyshyn, D.J., Stergiou, P., Lun, V.M., Meeuwisse, W.H., Worobets, J.T., 2006. Knee angular impulse as a predictor of patellofemoral pain in runners. Am. J. Sports Med. 34, 1844-1851.

Stoggl, T., Haudum, A., Birklbauer, J., Murrer, M., Muller, E., 2010. Short and long term adaptation of variability during walking using unstable (Mbt) shoes. Clin. Biomech. 25, 816-822.

Taube, W., Gruber, M., Gollhofer, A., 2008. Spinal and supraspinal adaptations associated with balance training and their functional relevance. Acta Physiol. (Oxf). 193, 101-116.

Wang, R., Gutierrez-Farewik, E.M., 2011. The effect of subtalar inversion/eversion on the dynamic function of the tibialis anterior, soleus, and gastrocnemius during the stance phase of gait. Gait Posture. 34, 29-35.

Winter, D.A., 1995. Human balance and posture control during standing and walking. Gait & Posture. 3, 193-214.

Winter, D.A., 1980. Overall principle of lower limb support during stance phase of gait. J. Biomech. 13, 923-927.

Zhang, S., Paquette, M.R., Milner, C.E., Westlake, C., Boyd, E., Baumgartner, L., 2012. An unstable rocker-bottom shoe alters lower extremity biomechanics during level walking. Footwear Sci. 4, 243-253.

Zhang, X., Paquette, M.R., Zhang, S., 2013. A comparison of gait biomechanics of flip-flops, sandals, barefoot and shoes. J. Foot Ankle Res. 6, 45-1146-6-45.

Table 1. Mean (SD) spatio-temporal and ankle, knee and hip joint kinematic variables measured during walking in an athletic shoe (KAL); FitFlop™ sandal (FF) and Birkenstock® Gizeh sandal (BIRK).

	KAL	BIRK	FF	pair-wise comparisons
Stance time (s)	0.63 (0.05)	0.62 (0.04)	0.63 (0.04)	
Step length (m)	0.75 (0.06)	0.74 (0.06)	0.74 (0.06)	
Ankle				
Sagittal				
Peak Plantarflexion (°)	-8.0 (2.9)	-4.3 (2.6)	-7.3 (2.1)	FF > BIRK***, KAL > BIRK***
Peak Dorsiflexion (°)	10.1 (2.6)	11.8 (2.7)	7.8 (2.8)	FF < KAL***, FF < BIRK***, KAL < BIRK***
ROM PF-DF (°)	18.1 (3.1)	16.1 (2.5)	15.1 (2.7)	FF < KAL***, KAL > BIRK***
Frontal				
Peak Abduction (°)	-2.6 (2.5)	-3.3 (2.9)	-3.6 (2.9)	
Peak Adduction (°)	6.2 (4.2)	3.3 (3.6)	4.1 (3.7)	FF < KAL**, KAL > BIRK**
ROM ABD-ADD (°)	8.8 (3.4)	6.6 (3.4)	7.6 (3.2)	FF < KAL*, FF > BIRK**, KAL > BIRK***
Transverse				
Peak External Rotation (°)	-1.4 (9.4)	-2.1 (10.0)	-2.3 (9.8)	
Peak Internal Rotation (°)	14.4 (9.6)	15.4 (10.1)	13.7 (9.9)	FF < BIRK**
ROM EXT-INT (°)	15.8 (4.6)	17.5 (5.0)	16.0 (4.8)	FF < BIRK**, KAL < BIRK**
Knee				
Peak Flexion (°)	-16.9 (6.4)	-18.1 (6.0)	-16.8 (6.4)	FF < BIRK***, KAL < BIRK***
ROM IC-KF (°)	-14.3 (4.0)	-14.2 (3.5)	-13.2 (3.7)	FF < KAL**, FF < BIRK*
Hip				
Peak Extension (°)	-15.1 (3.4)	-15.2 (3.4)	-15.1 (3.2)	
ROM IC-HE (°)	-38.5 (5.0)	-38.6 (5.4)	-38.1 (5.3)	

* denotes P<0.05, **P<0.01 and ***P<0.0001.

Table 2. Mean (SD) ankle, knee and hip joint moment variables measured during walking in an athletic shoe (KAL); FitFlop™ sandal (FF) and Birkenstock® Gizeh sandal (BIRK).

	KAL	BIRK	FF	pair-wise comparisons
Ankle				
Sagittal				
Peak DF Moment (Nm/kg)	0.200 (0.060)	0.203 (0.051)	0.177 (0.054)	FF < KAL*, FF < BIRK**
Time (% stance)	8.6 (1.1)	6.8 (1.3)	8.3 (1.5)	FF > BIRK***, KAL > BIRK***
Peak PF Moment (Nm/kg)	-1.414 (0.126)	-1.432 (0.120)	-1.348 (0.139)	FF < KAL**, FF < BIRK***
Time (% stance)	78.5 (1.7)	77.3 (1.7)	77.5 (3.5)	
Impulse (Nm/kg.s^{-1})	-0.316 (0.048)	-0.329 (0.045)	-0.304 (0.045)	FF < BIRK***, KAL < BIRK*
Frontal				
Peak ADD Moment (Nm/kg)	0.123 (0.031)	0.153 (0.047)	0.133 (0.039)	FF < BIRK*, KAL < BIRK***
Time (% stance)	39.1 (16.6)	33.7 (18.4)	28.4 (10.1)	FF < KAL**
Impulse (Nm/kg.s^{-1})	0.033 (0.018)	0.049 (0.022)	0.036 (0.021)	FF < BIRK**, KAL < BIRK***
Transverse				
Peak INT Moment (Nm/kg)	0.110 (0.039)	0.112 (0.041)	0.103 (0.032)	
Time (% stance)	11.4 (2.1)	10.6 (2.5)	11.5 (2.2)	
Peak EXT Moment (Nm/kg)	-0.660 (0.105)	-0.685 (0.117)	-0.649 (0.095)	FF < BIRK*
Time (% stance)	81.3 (2.0)	80.0 (1.7)	80.7 (1.7)	FF > BIRK*, KAL > BIRK***
Impulse (Nm/kg.s^{-1})	-0.127 (0.026)	-0.132 (0.025)	-0.122 (0.026)	FF < BIRK*
Total Negative Work (J.kg^{-1})	-0.168 (0.029)	-0.143 (0.021)	-0.128 (0.023)	FF < KAL***, FF < BIRK***, KAL > BIRK***
Total Positive Work (J.kg^{-1})	0.226 (0.041)	0.244 (0.048)	0.226 (0.043)	FF < BIRK*, KAL < BIRK**
Knee				
Peak KE Moment (Nm/kg)	0.433 (0.252)	0.475 (0.252)	0.422 (0.240)	FF < BIRK**, KAL < BIRK**
Time (% stance)	24.2 (2.5)	22.2 (1.6)	23.2 (3.8)	KAL > BIRK***
Peak KF Moment (Nm/Nm/kg)	-0.211 (0.118)	-0.236 (0.123)	-0.191 (0.111)	FF < BIRK**, KAL < BIRK**
Time (% stance)	63.2 (3.9)	62.5 (2.9)	60.1 (9.2)	
Impulse (Nm/kg.s^{-1})	0.051 (0.067)	0.049 (0.064)	0.050 (0.061)	
Hip				
Peak HE Moment (Nm/kg)	-1.215 (0.281)	-1.200 (0.278)	-1.270 (0.242)	FF > KAL*, FF > BIRK**
Time (% stance)	10.8 (2.4)	11.2 (2.4)	10.8 (2.3)	
Peak HF Moment (Nm/kg)	1.020 (0.213)	0.944 (0.195)	1.013 (0.187)	FF > BIRK***, KAL > BIRK***
Time (% stance)	86.7 (2.0)	85.6 (2.5)	86.3 (1.9)	KAL > BIRK*
Impulse (Nm/kg.s^{-1})	-0.027 (0.078)	-0.030 (0.072)	-0.037 (0.070)	FF > KAL*

* denotes $P<0.05$, $^{**}P<0.01$ and $^{***}P<0.0001$.

Figure 1. A: Microwobbleboard™ technology is a triple density midsole engineered from ethylene vinyl acetate (EVA) comprising a hard heel section (Shore A 45), a soft middle section (Shore A 27) and an intermediate density at the toe region (Shore A 35). **B**: The three

conditions tested (left to right): a standard commercially-available athletic trainer (KAL), a Birkenstock® Gizeh sandal (BIRK), and a FitFlop™ Walkstar sandal (FF). In KAL, windows for sensor placement were cut at the 1st and 5th metatarsal head regions and calcaneus (not visible).

Figure 2. Mean (*n*=28) joint angular kinematic profiles during stance phase. The shaded area represents the standard deviation bandwidth of the athletic shoe (KAL); the FitFlop™ sandal (FF) is denoted by the red line and the Birkenstock® Gizeh sandal (BIRK) by the thin black line.

Figure 3. Mean (*n*=28) joint moment ensemble profiles during stance phase. The shaded area represents the standard deviation bandwidth of the athletic shoe (KAL); the FitFlop™ sandal (FF) is denoted by the red line and the Birkenstock® Gizeh sandal (BIRK) by then thin black line.

Figure 4. Average anterior-posterior (A-P) and medio-lateral (M-L) centre of pressure (COP) trajectories normalised (a.u) to foot length (proximal to distal joint centre) and width (distal radius with respect to A-P axis), respectively. COP was expressed during early (0-33%), mid- (34-66%) and late (67-100%) stance phase regions between conditions. * denotes P<0.05, **P<0.01 and ***P<0.0001.

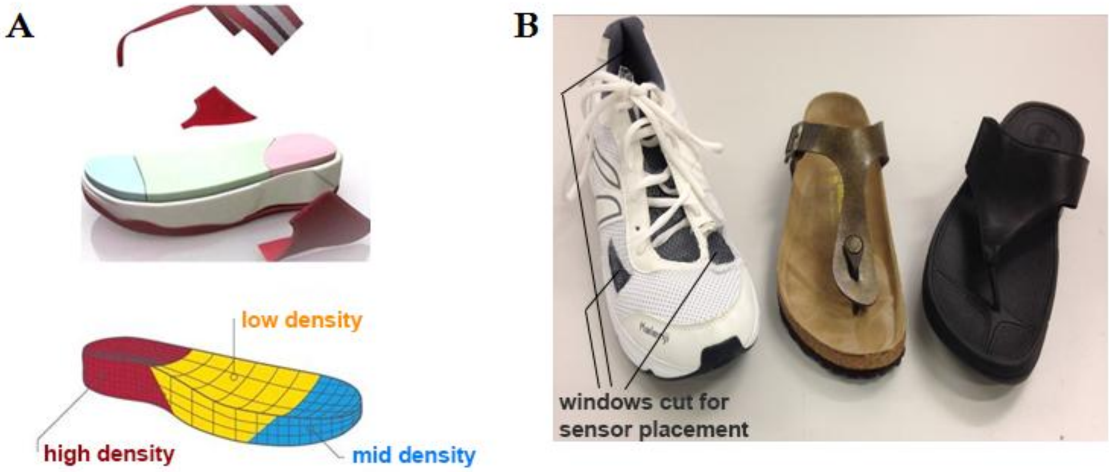
A
B
low density
high density
mid density
windows cut for
sensor placement

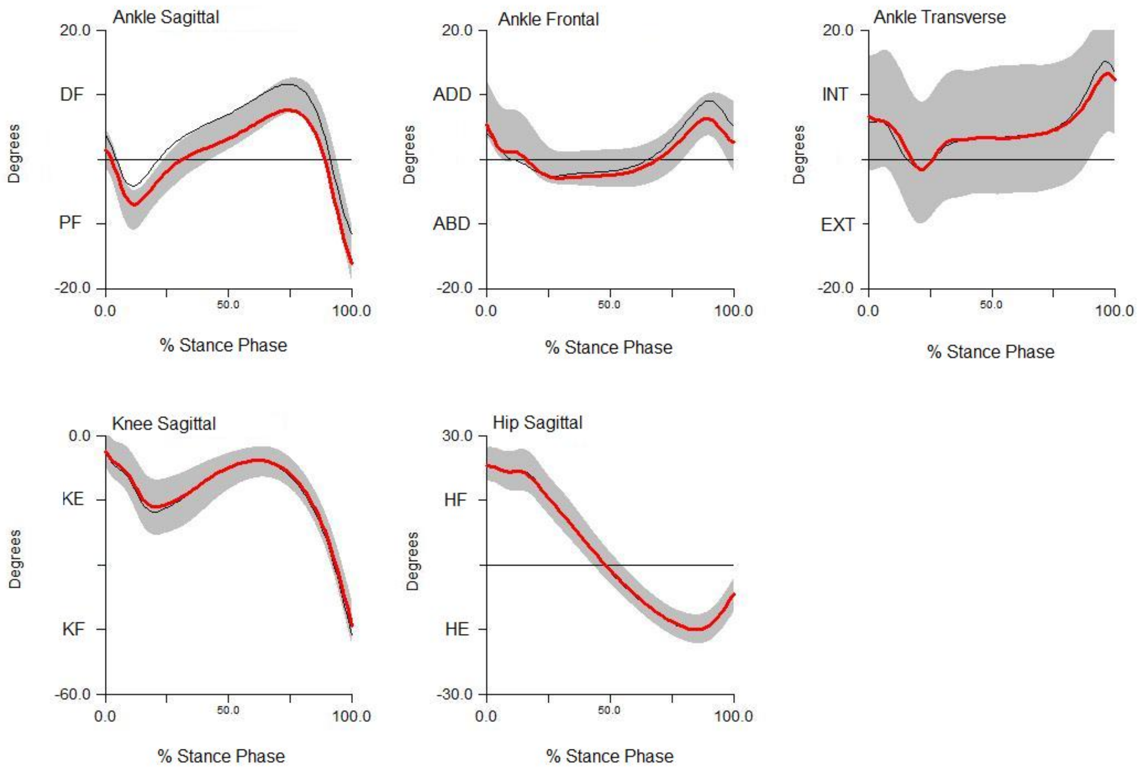
Ankle Sagittal
20.0
DF
PF
-20.0
Degrees
0.0
50.0
100.0
% Stance Phase
Ankle Frontal
20.0
ADD
ABD
-20.0
Degrees
0.0
50.0
100.0
% Stance Phase
Ankle Transverse
20.0
INT
EXT
-20.0
Degrees
0.0
50.0
100.0
% Stance Phase
Knee Sagittal
0.0
KE
KF
-60.0
Degrees
0.0
50.0
100.0
% Stance Phase
Hip Sagittal
30.0
HF
HE
-30.0
Degrees
0.0
50.0
100.0
% Stance Phase

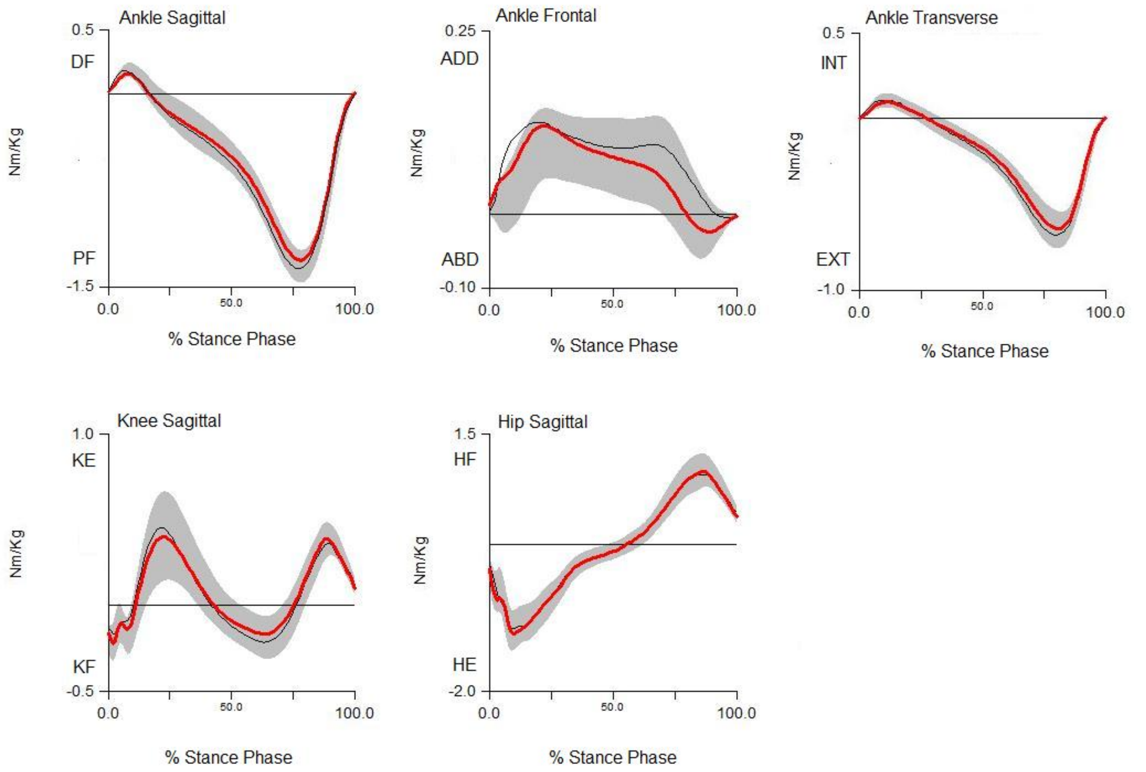
Ankle Sagittal
Ankle Frontal
Ankle Transverse
Knee Sagittal
Hip Sagittal
DF
PF
ADD
ABD
INT
EXT
KE
KF
HF
HE
Nm/Kg
% Stance Phase

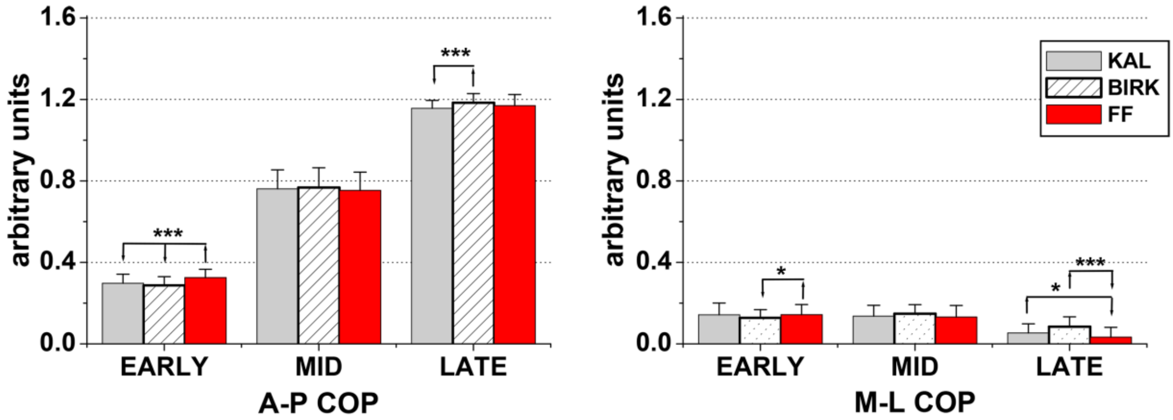
arbitrary units
EARLY
MID
LATE
A-P COP
M-L COP
KAL
BIRK
FF

Table 1
Click here to download high resolution image

	KAL	BIRK	FF	pair-wise comparisons
Stance time (s)	0.63 (0.05)	0.62 (0.04)	0.63 (0.04)	
Step length (m)	0.75 (0.06)	0.74 (0.06)	0.74 (0.06)	
Ankle				
Sagittal				
Peak Plantarflexion (°)	-8.0 (2.9)	-4.3 (2.6)	-7.3 (2.1)	FF > BIRK***, KAL > BIRK***
Peak Dorsiflexion (°)	10.1 (2.6)	11.8 (2.7)	7.8 (2.8)	FF < KAL***, FF < BIRK***, KAL < BIRK***
ROM PF-DF (°)	18.1 (3.1)	16.1 (2.5)	15.1 (2.7)	FF < KAL***, KAL > BIRK***
Frontal				
Peak Abduction (°)	-2.6 (2.5)	-3.3 (2.9)	-3.6 (2.9)	
Peak Adduction (°)	6.2 (4.2)	3.3 (3.6)	4.1 (3.7)	FF < KAL**, KAL > BIRK**
ROM ABD-ADD (°)	8.8 (3.4)	6.6 (3.4)	7.6 (3.2)	FF < KAL*, FF > BIRK**, KAL > BIRK***
Transverse				
Peak External Rotation (°)	-1.4 (9.4)	-2.1 (10.0)	-2.3 (9.8)	
Peak Internal Rotation (°)	14.4 (9.6)	15.4 (10.1)	13.7 (9.9)	FF < BIRK**
ROM EXT-INT (°)	15.8 (4.6)	17.5 (5.0)	16.0 (4.8)	FF < BIRK**, KAL < BIRK**
Knee				
Peak Flexion (°)	-16.9 (6.4)	-18.1 (6.0)	-16.8 (6.4)	FF < BIRK***, KAL < BIRK***
ROM IC-KF (°)	-14.3 (4.0)	-14.2 (3.5)	-13.2 (3.7)	FF < KAL**, FF < BIRK*
Hip				
Peak Extension (°)	-15.1 (3.4)	-15.2 (3.4)	-15.1 (3.2)	
ROM IC-HE (°)	-38.5 (5.0)	-38.6 (5.4)	-38.1 (5.3)	

Table 2

Click here to download high resolution image

	KAL	BIRK	FF	pair-wise comparisons
Ankle				
Sagittal				
Peak DF Moment (Nm/kg)	0.200 (0.060)	0.203 (0.051)	0.177 (0.054)	FF < KAL*, FF < BRK**
Time (% stance)	8.6 (1.1)	6.8 (1.3)	8.3 (1.5)	FF > BRK***, KAL > BRK***
Peak PF Moment (Nm/kg)	-1.414 (0.126)	-1.432 (0.120)	-1.348 (0.139)	FF < KAL**, FF < BRK***
Time (% stance)	78.5 (1.7)	77.3 (1.7)	77.5 (3.5)	
Impulse (Nm/kg.s^{-1})	-0.316 (0.048)	-0.329 (0.045)	-0.304 (0.045)	FF < BRK***, KAL < BRK*
Frontal				
Peak ADD Moment (Nm/kg)	0.123 (0.031)	0.153 (0.047)	0.133 (0.039)	FF < BRK*, KAL < BRK***
Time (% stance)	39.1 (16.6)	33.7 (18.4)	28.4 (10.1)	FF < KAL**
Impulse (Nm/kg.s^{-1})	0.033 (0.018)	0.049 (0.022)	0.036 (0.021)	FF < BRK**, KAL < BRK***
Transverse				
Peak INT Moment (Nm/kg)	0.110 (0.039)	0.112 (0.041)	0.103 (0.032)	
Time (% stance)	11.4 (2.1)	10.6 (2.5)	11.5 (2.2)	
Peak EXT Moment (Nm/kg)	-0.660 (0.105)	-0.685 (0.117)	-0.649 (0.095)	FF < BRK*
Time (% stance)	81.3 (2.0)	80.0 (1.7)	80.7 (1.7)	FF > BRK*, KAL > BRK***
Impulse (Nm/kg.s^{-1})	-0.127 (0.026)	-0.132 (0.025)	-0.122 (0.026)	FF < BRK*
Total Negative Work (J.kg^{-1})	-0.168 (0.029)	-0.143 (0.021)	-0.128 (0.023)	FF < KAL***; FF < BRK***, KAL > BRK***
Total Positive Work (J.kg^{-1})	0.226 (0.041)	0.244 (0.048)	0.226 (0.043)	FF < BRK*, KAL < BRK**
Knee				
Peak KE Moment (Nm/kg)	0.433 (0.252)	0.475 (0.252)	0.422 (0.240)	FF < BRK**, KAL < BRK**
Time (% stance)	24.2 (2.5)	22.2 (1.6)	23.2 (3.8)	KAL > BRK***
Peak KF Moment (Nm/Nm/kg)	-0.211 (0.118)	-0.236 (0.123)	-0.191 (0.111)	FF < BRK**, KAL < BRK**
Time (% stance)	63.2 (3.9)	62.5 (2.9)	60.1 (9.2)	
Impulse (Nm/kg.s^{-1})	0.051 (0.067)	0.049 (0.064)	0.050 (0.061)	
Hip				
Peak HE Moment (Nm/kg)	-1.215 (0.281)	-1.200 (0.278)	-1.270 (0.242)	FF > KAL*, FF > BRK**
Time (% stance)	10.8 (2.4)	11.2 (2.4)	10.8 (2.3)	
Peak HF Moment (Nm/kg)	1.020 (0.213)	0.944 (0.195)	1.013 (0.187)	FF > BRK***, KAL > BRK***
Time (% stance)	86.7 (2.0)	85.6 (2.5)	86.3 (1.9)	KAL > BRK*
Impulse (Nm/kg.s^{-1})	-0.027 (0.078)	-0.030 (0.072)	-0.037 (0.070)	FF > KAL*

Figure 1

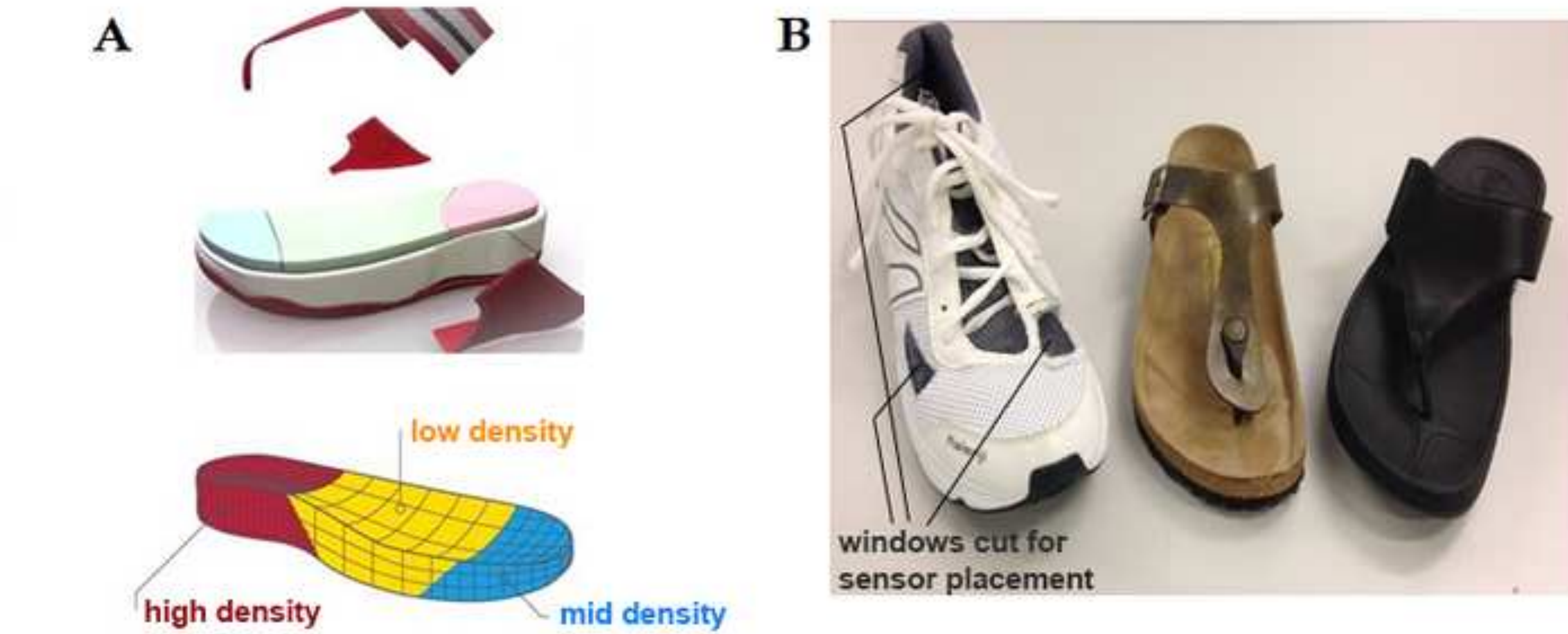
A
low density
high density
mid density
B
windows cut for
sensor placement

Figure 2
Click here to download high resolution image

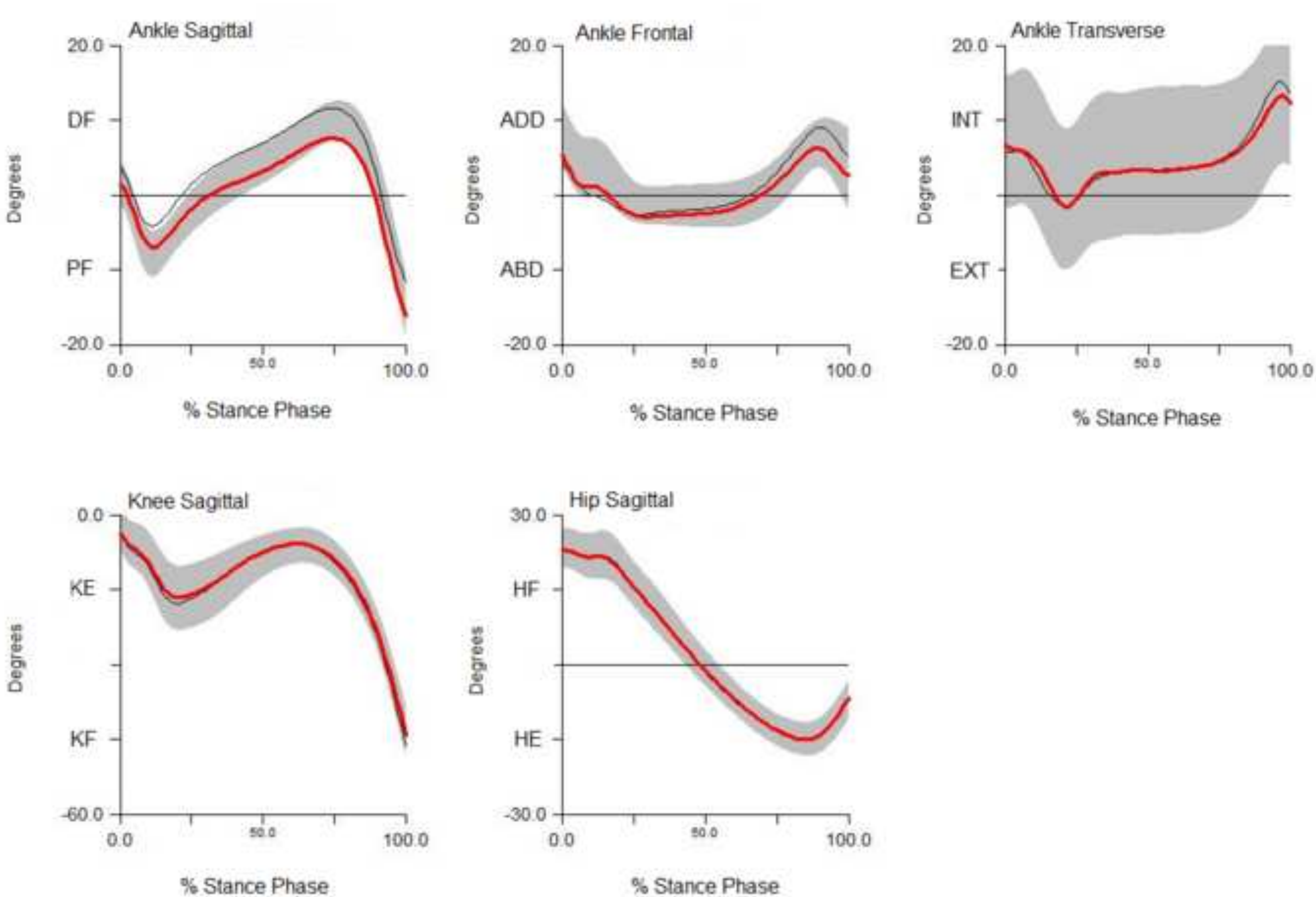

Figure 3
Click here to download high resolution image

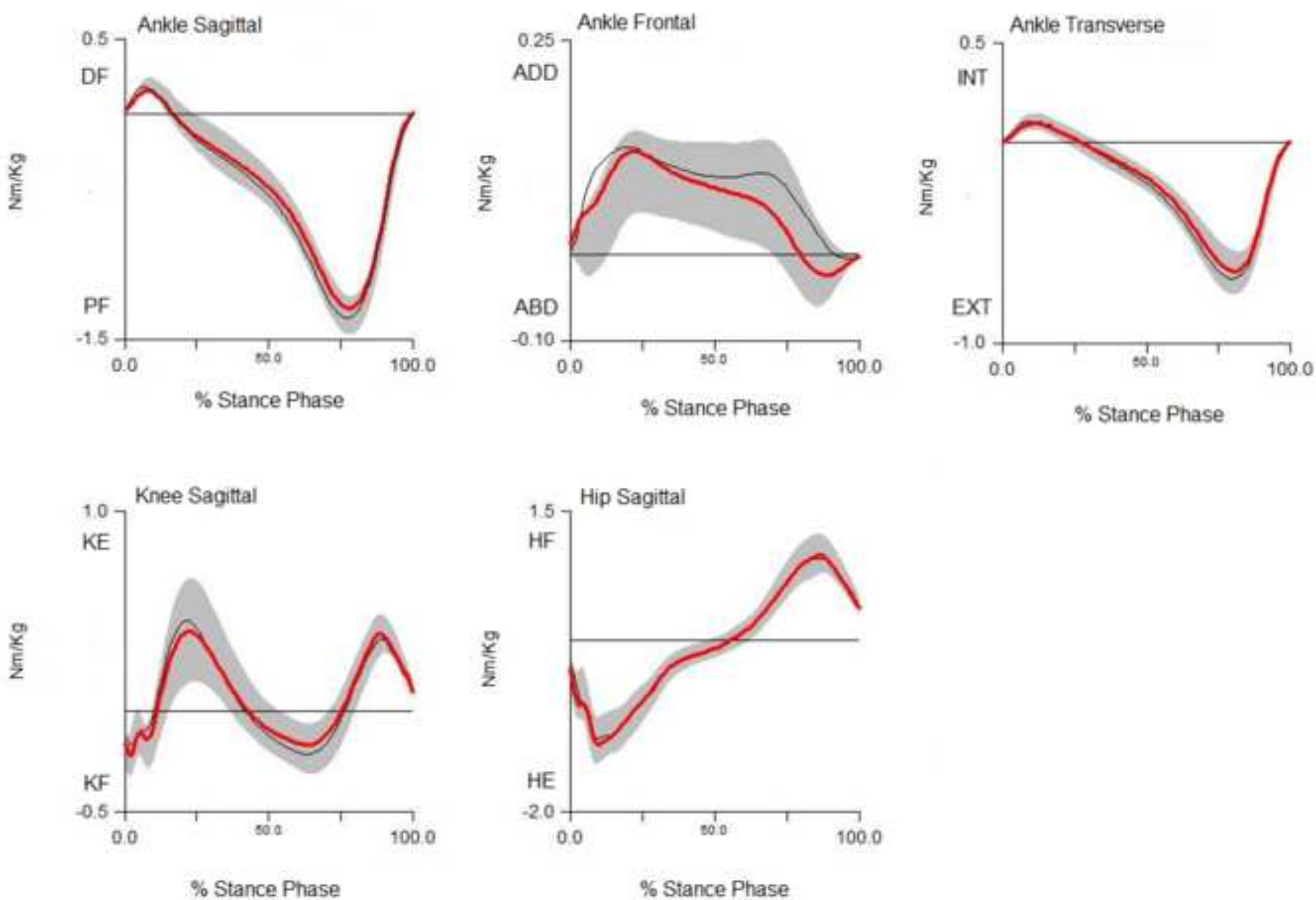

Figure 4
Click here to download high resolution image